Molecular Immunology 112 (2019) 30–39

Contents lists available at ScienceDirect

Molecular Immunology

journal homepage: www.elsevier.com/locate/molimm

BpV(pic) confers neuroprotection by inhibiting M1 microglial polarization and MCP-1 expression in rat traumatic brain injury

Rui Liu[a,b], Xin-Yu Liao[c], Jun-Chun Tang[b], Meng-Xian Pan[b], Song-Feng Chen[b], Pei-Xin Lu[d], Long J Lu[d], Zhi-Feng Zhang[e], Ying-Ying Zou[c], Li-Hong Bu[f,*], Xing-Ping Qin[a,*], Qi Wan[g,*]

[a] Department of Neurosurgery, Renmin Hospital of Wuhan University, 238 Jiefang Road, Wuhan, Hubei, 430060, China
[b] Department of Physiology, Collaborative Innovation Center for Brain Science, School of Basic Medical Sciences, School of Medicine, Wuhan University, 185 Donghu Street, Wuhan, Hubei, 430071, China
[c] Department of Pathology and Pathophysiology, Faculty of Basic Medical Sciences, Kunming Medical University, 1168 West Chunrong Road, Kunming, 650500, China
[d] School of Information Management, Wuhan University, Wuhan, Hubei, 430072, China
[e] Department of Physiology, School of Basic Medical Sciences, Hubei University of Medicine, Shiyan, Hubei, 442000, China
[f] PET-CT/MRI Center & Molecular Imaging Center, Renmin Hospital of Wuhan University, 99 Zhangzhidong Road, Wuchang district, Wuhan, Hubei, 430060, China
[g] Institute of Neuroregeneration & Neurorehabilitation, Department of Neurosurgery of the Affiliated Hospital, Qingdao University, 308 Ningxia Street, Qingdao, 266071, China

ARTICLE INFO

Keywords:
Traumatic brain injury
BpV(pic)
Microglia
Neuroinflammation
NF-κB p65
MCP-1

ABSTRACT

Traumatic brain injury (TBI) is a major cause of motor and cognitive impairment in young adults. It is associated with high mortality rates and very few effective treatment options. Bisperoxovanadium (pyridine-2-carboxyl) [bpV(pic)] is an commercially available inhibitor of Phosphatase and tensin homolog (PTEN). Previous studies have shown that bpV(pic) has protective effects in central nervous system. However, the role of bpV(pic) in TBI is unclear. In this study we aimed to investigate the neuroprotective role of bpV(pic) in rat TBI model. We found that injection of bpV(pic) significantly reduces brain edema and neurological dysfunction after TBI and this is mediated by AKT pathway. TBI is known to promote the M1 pro-inflammatory phenotype of microglial polarization and this effect is inhibited by bpV(pic) treatment which, instead promotes M2 microglial polarization in vivo and in vitro. We also found evidence of bpV(pic)-regulated neuroinflammation mediated by AKT activation and NF-κB p65 inhibition. BpV(pic) treatment also suppressed microglia in the peri-TBI region. MCP-1 is known to recruit monocytes and macrophages to promote inflammation, we show that bpV(pic) can inhibit TBI-induced up-regulation of MCP-1 via the AKT/NF-κB p65 signaling pathway. Taken together, our findings demonstrate that bpV(pic) plays a neuroprotective role in rat TBI, which may be achieved by inhibiting M1 microglia polarization and MCP-1 expression by modulating AKT/NF-κB p65 signaling pathway.

1. Introduction

Traumatic brain injury (TBI) is a leading cause of mortality and morbidity worldwide with few effective treatment options (Xiong et al., 2010). Approximately 10 million deaths per year and/or hospitalization are directly related to traumatic brain injury. Current treatment strategies rely on acute therapeutic intervention to reduce cell damage and brain edema (Narayan et al., 2002). Although we have a broad understanding of TBI, there has been no effective neuroprotective treatment to promote functional recovery after TBI. The inflammatory response is thought to be a key factor in the cascade of secondary injury after TBI. TBI induces a strong inflammatory response characterized by recruitment of peripheral leukocytes into brain parenchyma and activation of resident immune cells (Rhodes, 2011). TBI-induced microglial activation and subsequent release of pro-inflammatory cytokines such as tumor necrosis factor (TNF) and interleukins (IL), can lead to direct neuronal apoptosis(Guadagno et al., 2015). Moreover, these pro-inflammatory cytokines stimulate nitric oxide synthesis, leading to increased brain edema, brain damage, and further promote neuronal apoptosis(Corrigan et al., 2016; Guadagno et al., 2015).

Bisperoxovanadium (pyridine-2-carboxyl) [bpV(pic)] is an inhibitor of phosphatase and tensin homolog deleted on chromosome 10 (PTEN) (Liu et al., 2017). PTEN is a tumor suppressor, which plays an important role in intracellular signal transduction that mediates cell proliferation and survival (Wang et al., 2015). PTEN has two activities of lipid phosphatase and protein phosphatase (Poon et al., 2010). The

* Corresponding authors.
E-mail addresses: bulihongs@whu.edu.cn (L.-H. Bu), qxp718@whu.edu.cn (X.-P. Qin), qiwanwh@foxmail.com (Q. Wan).

https://doi.org/10.1016/j.molimm.2019.04.010
Received 6 August 2018; Received in revised form 8 April 2019; Accepted 23 April 2019
Available online 08 May 2019
0161-5890/

function of bpV(pic) is to inhibit PTEN lipid phosphatase activity (Chen et al., 2015). PTEN lipid phosphatase activity is always associated with AKT activation, during inhibition of the lipid phosphatase activity of PTEN. AKT activation exhibits neuroprotection in many neuropathological conditions (Makker et al., 2014). Previous studies have demonstrated that neuronal AKT can be activated by bpV(pic) to reduce neuronal death in ischemic stroke injury (Shi et al., 2011). Althrough the neuroprotective effect of bpV(pic) has been extensively studied, its' role in TBI remains larger unclear.

In this study, our results indicate that bpV(pic) exhibits neuroprotection in rat TBI through AKT activation. We show that bpV(pic) inhibits M1 microglial polarization after TBI by activation of AKT and subsequent inhibition of NF-κB p65. BpV(pic) also suppresses the expression of MCP-1 by regulating the AKT/NF-κB p65 signaling pathway, thereby attenuating inflammation.

2. Materials and methods

2.1. Animals

Adult male Sprague-Dawley (SD) rats were given free water and food in a temperature-controlled room (23–25 °C) with 12-hour light/dark cycle, 3 mice per cage. Animals were allowed to adapt to the environment for at least 3 days before the experiment. In our in vivo experiments, we used a total of 324 male rats and discarded 23 male rats during surgery. 9 adult pregnant female rats and 46 embryos were used in our cortical microglia culture experiments. All animal use and experimental protocols were approved and implemented according to the IACUC guidelines and the animal care and ethics committee of the Wuhan University School of Medicine. Samples to experimental groups and collecting and processing data are randomly assigned. Experiments were conducted by researchers who did not know the group to which each animal was assigned.

2.2. Traumatic brain injury model

Traumatic brain injury was induced by Feeney's weight-drop method, with slight modifications (Feeney et al., 1981; Wang et al., 2011). Adult male SD rats (250–280 g) were intraperitoneally anesthetized with 2% pentobarbital (30 mg/kg) and maintained at 37 °C using a water heating pad throughout the procedure. The rats' heads were immobilized in a stereotactic frame, and a right parietal craniotomy (3.5 mm posterior and 2.5 mm lateral to bregma, 4 mm in diameter) was conducted with a drill under aseptic conditions. A flat-ended steel rod (3.5 mm in diameter, 25 g) was allowed to free fall from a height of 30 cm onto a piston resting on the dura. The piston was allowed to compress the brain tissue to a depth of 2.5 mm and produce moderate brain injury. Sham-operated animals were anesthetized and subjected to identical surgical procedures, but not weight-drop brain injury. Sham-operated rats underwent the same craniotomy without cortical effects. After the operation, all rats were returned to housing in random groups, and the room temperature was maintained at 37 ± 0.5 °C.

2.3. Brain water content measurements

Brain water content was measured 72 h after TBI. After anesthesia and decapitation, the brain was immediately excised and divided into two hemispheres along the midline, and the cerebellum was removed. The same side hemisphere was placed on pre-weighed aluminum foil to give a wet weight, and then dried in an electric oven at 100 °C for 24 h. The percentage of brain water is calculated as follows: (wet weight - dry weight)/(wet weight) (Chen et al., 2017b).

2.4. Neurological severity score test

The rats were received a previously reported modified neurological severity score test. These tests are a series of reflexes, feelings, movements and balance tests similar to the human contralateral neglect test. Neurological function score from 0 to 18 (normal score, 0; maximum deficit, 18) (Chen et al., 2001).

2.5. Morris water maze test

The MWM test was conducted according to the previously described method (Bromley-Brits et al., 2011; Majkutewicz et al., 2016). We have used a black circular pool with a diameter of 150 cm and a depth of 60 cm A black and white analog video camera was connected to a video-tracking digitizing device (EthoVision XT, Noldus, Netherlands). The specific navigation cue (white round paper spot) was provided to compensate for impaired visual acuity in albino rats strains. Animals were trained for the MWM task as follows: in the center of one quadrant, a transparent, cylindrical and plexiglass platform (10 cm) was placed 1 cm above the water surface. The rat was released in the quadrant opposing the platform with its head directed towards the wall of the pool. If the rat did not locate the platform after 60 s, it was gently steered towards the platform by hand and allowed to stay there for 10 s before returning to its home cage. If the rat found the platform before 60 s cut-off, it was allowed to stay on the platform for additional 5 s and then returned to its home cage.

Reference memory version of the MWM test was performed according to Olton and Santos with some modifications. In this study, the platform was hidden 1–2 cm below the surface of the water and located in a single, fixed position in the center of the critical quadrant (CQ). The rat was placed near the border of the pool with its head directed towards the wall of the pool. During each trial rat swam until it located and climbed onto the platform (latency measurement), or until 120 s had elapsed. If the rat did not find the platform within 120 s, it was manually guided to the platform and allowed to remain on it for a 10 s period, in this case a maximum latency of 120 s was assigned. The following parameters were measured: latency to reach the platform, distance swum to reach the platform, percent of time spent in the CQ of the pool (where the platform was located), frequency in the CQ and the overall velocity.

Each animal was exposed to four trials per session (one session day), with an inter-trial interval of 10 min for four consecutive days. Acquisition of the reference memory task was denoted by a decrease in a distance swum, an increase in the percent time spent in the CQ and increase in the overall velocity. At the end of the reference memory acquisition phase, on the fifth day, a probe test was conducted with the platform removed. During this test, animals were allowed to swim freely in the pool for 120 s. The following parameters were measured: latency to reach the critical annulus (the virtual contour of the removed platform), the percent time spent in the CQ, and the frequency in the CQ.

2.6. Immunofluorescence analysis

The immunofluorescence staining steps based on the description of the prior execution (Mason et al., 2000). The brain sections were treated with primary antibody rabbit anti- phospho-AKT (Ser473) (1:250) from Cell Signaling Technology, mouse anti- Iba-1 (1:250) from Abcam. The secondary antibody goat anti- Rabbit 594, goat anti- Mouse 488 from Molecular Probes (Eugene, USA). The hochest probe from Life Technologies. The sections were photographed by a blinded investigator using an Olympus fluorescent microscope (IX51, Olympus, Japan). Analysed by Image J software (Image J, USA).

2.7. Western blotting analysis

Western blotting was performed as previously described (Chen et al., 2017a). Briefly, the polyvinylidene difluoride (PVDF) membrane by Millipore (USA) was used incubate with a first antibody against AKT (Mouse, 1:1000), phospho-AKT (Ser^{473}) (Rabbit, 1:2000), NF-κB p65 (Rabbit, 1:1000), Actin (Rabbit, 1:2000) from Cell Signaling Technology (MA, USA), Iba-1 (Mouse, 1:500) from Abcam, MCP-1 (Rabbit, 1:1000) from Proteintech. First antibodies were labelled with secondary antibody, protein bands were imaged using SuperSignal West Femto Maximum Sensitivity Substrate (Pierce, Rockford, IL, USA). The EC3 Imaging System (UVP, LLC, Uplant, USA) was used to obtained blot images directly from the PVDF membrane. The data of western blot were quantified using Image-Pro Plus Version 6.0, USA.

2.8. qRT-PCR

Total RNA was isolated from pseudo-brain and ischemic brains using the RNeasy Mini Kit (Qiagen) according to the manufacturer's instructions; the first strand of cDNA was synthesized using 5 μg of Superscript First-Strand Synthesis System (Invitrogen) for qRT-PCR. PCR was performed on the Opticon 2 real-time PCR detection system (Bio-Rad) using the corresponding primers (Table 1) and SYBR gene PCR master mix (Invitrogen). The cycle time value was normalized to GAPDH of the same sample. The mRNA expression level was then reported as a fold change compared to the control group.

2.9. Cortical microglia culture

Cortical microglia cultures were prepared from female SD rats at 17 days of gestation. Pregnant rats died of cervical dislocation after anesthesia with 4% isoflurane with 70% N_2O and 30% O_2. Embryos were sprayed with 70% ethanol and removed after rats. The embryos were quickly removed, the embryo skulls were removed, and the brain tissue was completely removed. Pelleted cells were resuspended in warmed DMEM culture medium completed with 10% heat inactivated FBS, 1% antibiotic-antimycotic, and 5 ng/ml carrier-free recombinant mouse GM-CS and counted. 1.3×10^6cells were seeded into tissue culture grade poly L-lysine coated T75 cell culture treated flasks and placed in a 37 °C incubator with relative humidity. Culture supernatant was replaced twice weekly with 10 ml fresh completed medium until confluency of cells was observed, at approximately three weeks.

2.10. Intraventricular injection (i.c.v) administration

Rats were anesthetized with a mixture of 4% isoflurane in 30% O_2 and 70% N_2O in a sealed see-through box. When the rats are deeply anesthetized, we will use the ear bars and upper incisor rods to fix the rat's head in a stereo frame and continue the anesthesia of the rats with 4% isoflurane using a mask. Next, make a small sagittal incision and use the anterior fontanelle as an anatomical reference point. The ventricles (from the anterior fontanelle: lateral, 1.5 mm; anterior-posterior, -0.8 mm; depth, 3.5 mm) were used with a 23 gauge needle connected to a Hamilton microsyringe via a polyethylene tube, and at 1.0 l/minute. The correct needle placement was confirmed by taking a few micrograms of clear cerebrospinal fluid from the Hamilton micro-syringe.

2.11. Treanment

Animals were dosed with bpV(pic) 4 times at a dose of 20 μg/100 g, injected intraperitoneally 3 h apart, and ischemia was induced 20 min after the last injection. AKT inhibitor IV (100 μM, 2 μL) was used 1 h before treatment of bpV(pic) by i.c.v (Supplementary Fig. 1).

On the day of treatment, microglia was treated with bpV(pic) (200 nM) 1 h before LPS treatment, and AKT inhibitor IV (1 μM) or the anti-inflammatory agent Helenalin (2 μM) was treated 1 h before bpV (pic) treatment. The cells were then collected for western blot analysis.

2.12. Statistics

In this study, on experimental design and analysis, the data and statistical analysis comply with the recommendations. All datas are expressed as mean ± SE. Student's *t*-test, variance analysis, mann-whitney u and friedmann's test was used in differences among groups. $P < 0.05$ was considered statistically significant.

3. Results

3.1. BpV(pic) treatment reduces brain water content and promotes functional recovery after TBI

Traumatic brain injury is defined as brain damage caused by external mechanical forces, including acceleration, deceleration, and rotational forces. To inverstigate the potential neuroprotective effects of bpV(pic) on TBI, we used a modified Feeney's weigh-drop method to induce experimental TBI model in rats. As shown in Fig. 1a, the percentage of water content of rat brain was significantly increased after 72 h of TBI, and this was partly prevented by bpV(pic) treatment. In addition, to assess the systemic administration effects of bpV(pic) after TBI, the modified neurological severity score (mNSS) and Morris water maze test (MWM) were performed in rats at indicated time point after TBI. Results showed that bpV(pic) treatment improved neurological function in rats after TBI (Fig. 1b–e). Together, treatment of bpV(pic) reduces brain water content and promotes functional recovery in rats after TBI.

3.2. BpV(pic)-induced neuroprotection after TBI is mediated by activation of AKT

BpV(pic) can activate AKT by inhibiting PTEN (Chen et al., 2015). Previous studies have demonstrated that activation of AKT plays a neuroprotective role in neuropathological conditions (Zhang et al., 2016). Western blotting analysis of the S473 phosphorylation of AKT (p-AKT) in the cortex of peri-TBI region showed that the level of p-AKT was down-regulated at the indicated time point after TBI (Sham; TBI

Table 1
Primers for qRT-PCR.

Gene	Primer
M1	
IL-1β	SENS: GAGGACATGAGCACCTTCTTT REVS: GCCTGTAGTGCAGTTGTCTAA
TNF-α	SENS: ACCACGCTCTTCTGTCTACT REVS: GTTTGTGAGTGTGAGGGTCTG
CD32	SENS: AATCCTGCCGTTCCTACTGATC REVS: GTGTCACCGTGTCTTCCTTGAG
M2	
Arg-1	SENS: TCACCTGAGCTTTGATGTCG REVS: CTGAAAGGAGCCCTGTCTTG
IL-10	SENS: AAATAAGAGCAAGGCAGTGG REVS: GTCCAGCAGACTCAATACACA
TGF-β	SENS: TGCGCTTGCAGAGATTAAAA REVS: CGTCAAAAGACAGCCACTCA

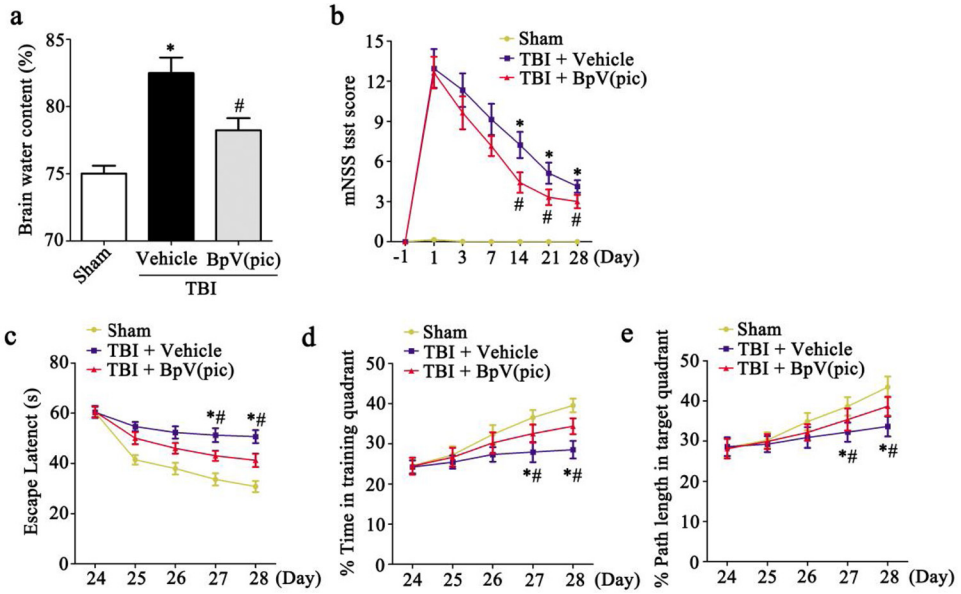

Fig. 1. BpV(pic) treatment reduces brain water content and promotes functional recovery after TBI.

(a) BpV(pic) treatment decreased brain water content 3 days after TBI (n = 6 at each group, $^{*}P < 0.05$ versus the Sham, $^{\#}P < 0.05$ versus the TBI + Vehicle). Statistical analysis was implemented by student's *t*-test and variance analysis. (b) Rats treated with bpV(pic) have lower scores in mNSS test at indicated time point after TBI compared with I/R + Vehicle group (n = 15 at each group, $^{*}P < 0.05$ versus the Sham, $^{\#}P < 0.05$ versus the TBI + Vehicle). Statistical analysis was implemented by mann-whitney u and friedmann's test. (c–e) Morris water maze test were significantly improved by bpV(pic) (n = 15 at each group, $^{*}P < 0.05$ versus the Sham, $^{\#}P < 0.05$ versus the TBI + Vehicle). Statistical analysis was implemented by mann-whitney u and friedmann's test. Datas are expressed as mean ± SE.

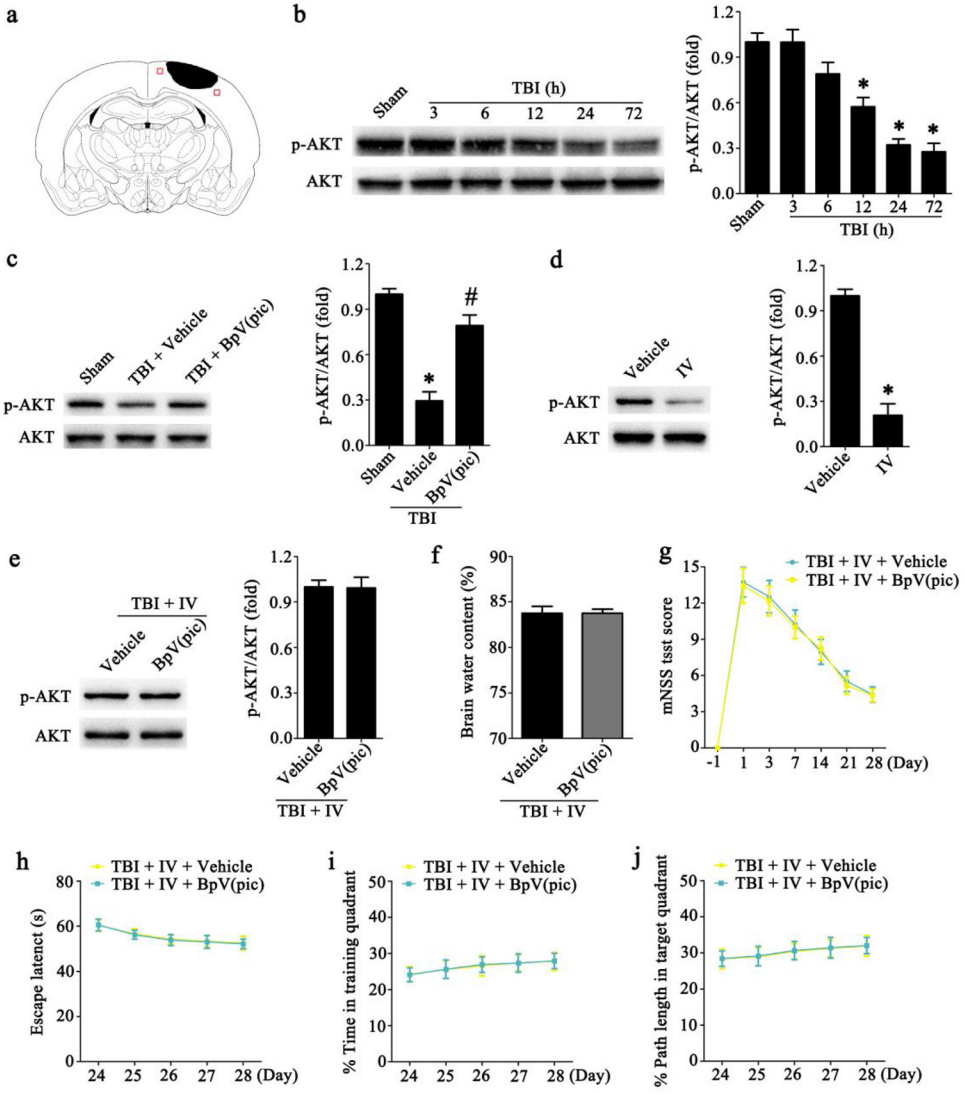

Fig. 2. BpV(pic)-induced neuroprotection after TBI is mediated by activation of AKT in rats.

(a) Diagram of a coronal rat brain section showing the relationship of the lesion cavity (black) to the peri-TBI region (red squares). (b) Western blotting analysis of p-AKT at indicated time point after TBI in rats showed that the leve of p-AKT decreased after TBI (n = 6 at each group, $^{*}P < 0.05$ versus the Sham). (c) Western blotting analysis of p-AKT after TBI in rats showed that bpV(pic) treatment increased the level of p-AKT (n = 6 at each group, $^{*}P < 0.05$ versus the Sham, $^{\#}P < 0.05$ versus the TBI + Vehicle). (d) Western blotting analysis of p-AKT showed that IV treatment decreased the level of p-AKT (n = 6 at each group, $^{*}P < 0.05$ versus the Vehicle). (e) Western blotting analysis of p-AKT after TBI in rats when pretreated with IV showed that bpV(pic) treatment did not increase the level of p-AKT (n = 6 at each group). (f) Brain water content had no significant difference 3 days after TBI + IV when treatment of bpV(pic) (n = 6 at each group). (g) Rats treated with bpV(pic) had no significant difference in mNSS test at indicated time point after TBI + IV (n = 6 at each group). (h–j) Morris water maze test had no significantly improved by bpV(pic) after TBI + IV (n = 6 at each group). Datas are expressed as mean ± SE. Statistical analysis was implemented by student's *t*-test and variance analysis.

3 h, 6 h, 12 h, 24 h, 72 h) (Fig. 2a and b). After treatment of bpV(pic), the level of p-AKT increased compared with TBI + Vehicle at 24 h after TBI (Fig. 2c). Furthermore, we injected AKT inhibitor IV (100 μM, 2 μL) by i.c.v 1 h before treatment of bpV(pic) in rats (Fig. 2d). Western blotting analysis of p-AKT showed that the level of p-AKT had no significant difference in the case of bpV(pic) treatment after 24 h of TBI (Fig. 2e). Meanwhile, the percentage of brain water content in rats did not show significant differences in the treatment of bpV(pic) after inhibition of AKT (Fig. 2f). And neither the bpV(pic)-induced neurological function recovery was observed (Fig. 2g–j). Together, these results suggest that bpV(pic)-induced neuroprotection after TBI in rats is mediated by AKT activation.

3.3. BpV(pic) inhibits TBI-induced M1 microglial polarization

Neuroinflammation is thought to be a key factor in the cascade of secondary injury after TBI (Kumar and Loane, 2012). Microglia is an innate immune cell in the CNS and a major mediator of neuroinflammation (Czeh et al., 2011). Microglia is characterized by resident macrophages, which can be activated as M1 microglia (classically activated) and M2 microglia (alternatively activated) (Tam and Ma, 2014). The M1 phenotype of microglia shows pro-inflammatory effects and M2 microglia shows anti-inflammatory. There are several markers of M1 and M2 phenotypes, which are sensitive but not specific. We therefore used numerous markers of M2 microglia to increase our specificity of the M2 phenotype. These markers included IL-1β, TNF-α and CD32 as the markers of M1 microglia, *Arg-1*, *IL-10* and *TGF-β* (Benson et al., 2015). Using qRT-PCR analysis of M1 and M2 microglial markers we showed that IL-1β, TNF-α and CD32 significantly increased at 24 h after TBI, and the TBI-induced mRNA levels of *IL-1β*, *TNF-α* and *CD32* up-regulation were reduced with treatment of bpV(pic) (Fig. 3a). Meanwhile, the mRNA levels of *Arg-1*, *IL-10* and *TGF-β* were up-regulated by bpV(pic) treatment (Fig. 3b). These results suggest that treatment of bpV(pic) inhibits M1 microglial polarization and promotes anti-inflammatory after TBI.

3.4. BpV(pic) regulates microglial polarization by activating AKT

To further explore whether bpV(pic)-regulated neuroinflammation is mediated by AKT activation, we performed double-immunofluorescence staining of p-AKT and Iba-1 in the cortex of peri-TBI area. Results show that the level of microglial p-AKT was reduced following TBI and this process was reversed with bpV(pic) treatment (Fig. 4a and b). There were no significant differences in M1 and M2 microglial markers after IV bpV(pic) treatment (Fig. 4c and d). These results suggest that bpV(pic) promotes anti-inflammatory by regulating AKT activation. Furthermore, we introduced LPS-treated cultured cortical microglia to mimic M1 microglial polarization after TBI (Xu et al., 2015). The level of p-AKT decreased after LPS treatment and was up-regulated by bpV(pic) (Supplementary Fig. 2a). qRT-PCR showed that M1 markers significantly increased after LPS treatment and this process was reduced by treatment of bpV(pic) (Supplementary Fig. 2b and c). Meanwhile, bpV(pic)-mediated LPS-induced microglial polarization was also reduced by treatment of AKT inhibitor IV (Supplementary Fig. 3a–c). Support our results *in vivo*.

3.5. NF-κB p65 mediates bpV(pic)-regulated neuroinflammation

Previous studies have shown that NF-κB p65 plays a major role in inflammation and may be a potential downstream mediator of AKT-mediated inflammation (Yuan et al., 2016; Zhang et al., 2012). Western blotting analysis of NF-κB p65 showed that TBI and LPS increased the level of p65 *in vivo* and *in vitro* (Fig. 5a and b), and treatment of bpV (pic) decreased the level of p65 (Fig. 5a and b), meanwhile, a contrary result was seen in IkB phosphorylation levels (Fig. 5c and d). We also tested the level of p65 in the nucleus, and showed that bpV(pic) reduced the upregulation of p65 level in the nucleus induced by TBI (Fig. 5e and f). We subsequently pre-treated microglia with the p65 inhibitor Helenalin (2 μM) 1 h before LPS (Fig. 5g). qRT-PCR analysis of M1 and M2 markers showed that bpV(pic)-regulated neuroinflammation were not observed (Fig. 5h and i). These results suggest that bpV (pic)-regulated neuroinflammation is mediated by p65. To explore whether bpV(pic)-regulated p65 is dependent on AKT activation, we first confirmed the relationship between p65 and AKT. Inhibition of AKT increased the level of p65 in cultured cortical microglia, whereas suppression of p65 did not show significant differences in p-AKT levels (Fig. 5j and k). After pre-treat microglia with AKT inhibitor IV, we performed western blotting analysis and show that bpV(pic)-induced

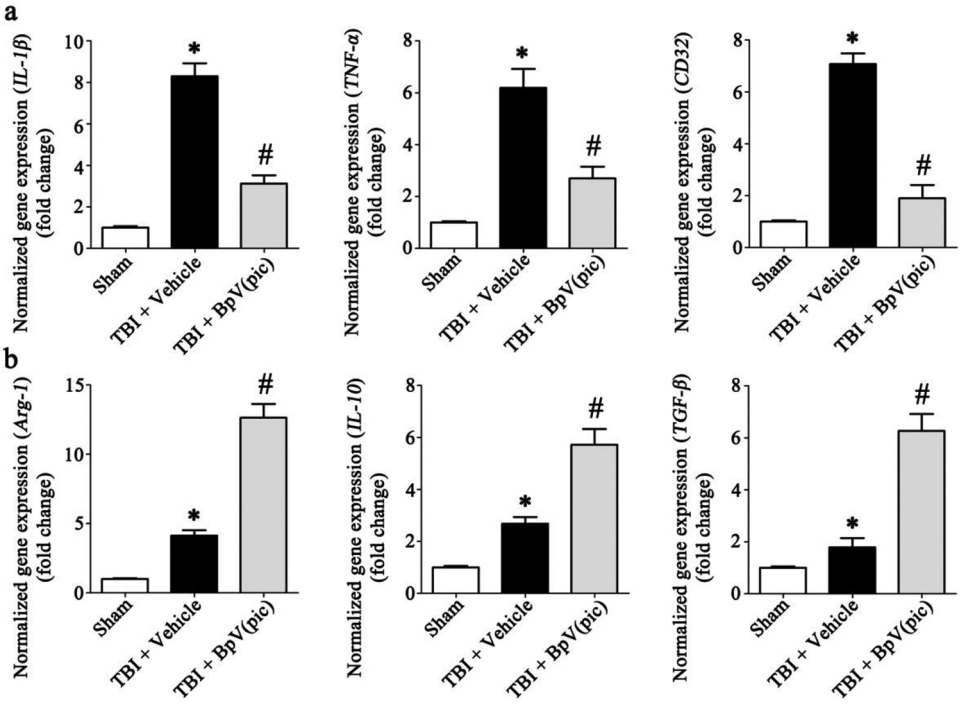

Fig. 3. BpV(pic) inhibits TBI-induced M1 microglial polarization.
(a) qRT-PCR analysis of M1 microglia markers IL-1β, TNF-α and CD32 in rats 72 h after TBI, showed that TBI increased the mRNA levels of *IL-1β*, *TNF-α* and *CD32* compared with Sham and bpV(pic) treatment down-regulated the mRNA levels of *IL-1β*, *TNF-α* and *CD32* compared with TBI + Vehicle (n = 6 at each group, $^{*}P < 0.05$ versus Sham, $^{\#}P < 0.05$ versus TBI + Vehicle). (b) qRT-PCR analysis of M2 microglia markers Arg-1, IL-10 and TGF-β in rats 72 h after TBI, showed that the mRNA levels of *Arg-1*, *IL-10* and *TGF-β* have no significant up-regulation after TBI compared with Sham and bpV(pic) treatment significantly up-regulated the mRNA levels of *Arg-1*, *IL-10* and *TGF-β* compared with TBI + Vehicle (n = 6 at each group, $^{*}P < 0.05$ versus Sham, $^{\#}P < 0.05$ versus TBI + Vehicle). Datas are expressed as mean ± SE. Statistical analysis was implemented by student's *t*-test and variance analysis.

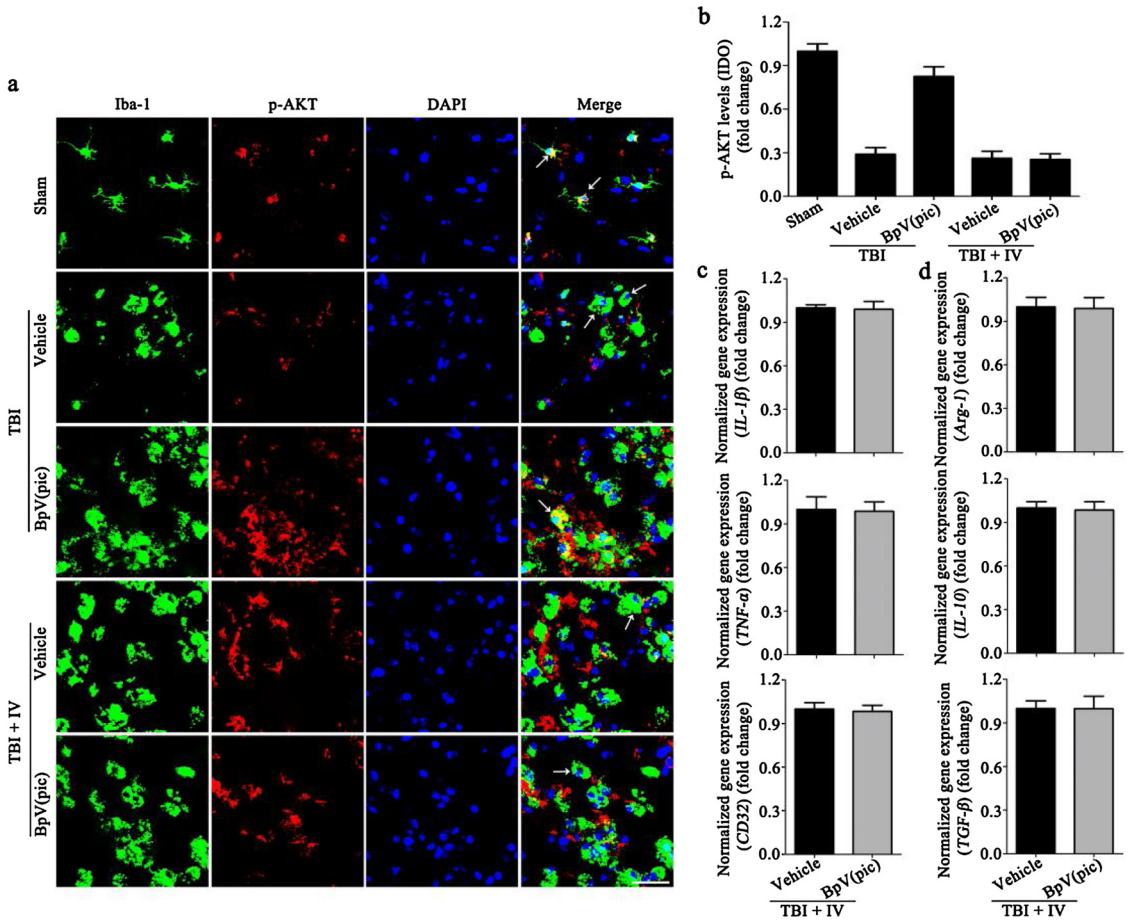

Fig. 4. BpV(pic)-regulated microgial polarization is mediated by AKT activation.
(a) Double-immunofluorescence staining of p-AKT (red) with Iba-1 (green) in the cortex of peri-TBI region 72 h after TBI showed that the level of p-AKT increased by bpV(pic) treatment after TBI. Scale bar, 20 μm. (b) The optical density (OD) analysis of p-AKT levels (n = 6 at each group, $^*P < 0.05$ versus Sham TBI + Vehicle). (c) qRT-PCR analysis of M1 microglia markers IL-1β, TNF-α and CD32 in rats 72 h after TBI + IV, showed that the mRNA levels of *IL-1β*, *TNF-α* and *CD32* had no significant difference after bpV(pic) treatment (n = 6 at each group). (d) qRT-PCR analysis of M2 microglia markers Arg-1, IL-10 and TGF-β in rats 72 h after TBI + IV, showed that the mRNA levels of *Arg-1*, *IL-10* and *TGF-β* had no significant difference after bpV(pic) treatment (n = 6 at each group). Datas are expressed as mean ± SE. Statistical analysis was implemented by student's *t*-test and variance analysis.

p65 down-regulation does not occur (Fig. 5l). These results indicate that bpV(pic)-regulated p65 is mediated by AKT activation. BpV(pic) down-regulates p65 by activating AKT, thereby inhibiting M1 microglial polarization and promoting the pro-inflammatory state.

3.6. BpV(pic) alleviates the increase of microglia in TBI lesion region

Previous studies have demonstrated that up-regulation of the number of microglia in injured region is also one of the main causes of neuroinflammation after TBI (Loane and Kumar, 2016). Western blotting analysis of microglial marker Iba-1 showed significant upregulation of Iba-1 levels in the peri-TBI region after TBI, which was reduced by bpV(pic) treatment (Fig. 6a). These results were further supported by immunofluorescence stain results (Fig. 6b and c). These results suggest that TBI-induced increase of microglia in the lesion region can be alleviated by bpV(pic). Monocyte chemotactic protein-1 (MCP-1) is known to recruit monocytes and macrophages to promote inflammation (Sawyer et al., 2014). We analyzed the level of MCP-1 in peri-TBI region 24 h after TBI, and observed that the level of MCP-1 increased after TBI and bpV(pic) treatment reduced TBI-induced MCP-1 up-regulation (Fig. 7a and b). A similar finding was seen in LPS-treated microglia (Fig. 7c and d). To further explore the mechanism of bpV(pic)-regulated MCP-1 expression, we also tested the level of MCP-1 in cultured cortical microglia after treatment of AKT inhibitor IV or Helenalin. Results showed that inhibition of AKT increased the expression of MCP-1, whereas Helenalin reversed this (Fig. 7e and f), meanwhile, bpV(pic) treatment did not show significant differences in MCP-1 levels (Fig. 7g and h). These results suggest that bpV(pic)-regulated MCP-1 expression is mediated by AKT/p65 signaling pathway. We therefore conclude that bpV(pic)-mitigated microglia increase in TBI lesions by inducing MCP-1 upregulation.

4. Discussion

PTEN is a tumor supressor and plays an important role in mediating intracellular signaling of cell proliferation and survival (Milella et al., 2015; Muniyan et al., 2014). Previous studies from us and others have shown that inhibition of PTEN confers neuroprotective effect in ischemic stroke injury (Chen et al., 2016; Zhang et al., 2017). BpV(pic) is a commercially available PTEN inhibitor. We have widely known that bpV(pic) plays a neuroprotective role in the activation of AKT by inhibiting PTEN lipid phosphatase activity in neurons after ischemic stroke (Liu et al., 2010; Tian et al., 2012). However, the role of bpV(pic) in TBI is un clear. Here, we demonstrate that bpV(pic) exhibits neuroprotection after TBI in rats, which may be mediated by inhibition of M1 microglia polarization and MCP-1 expression by regulating AKT/NF-κB p65 signaling pathway.

TBI is a major cause of global mortality and morbidity (Xiong et al., 2010). TBI-induced brain damage is mainly manifested as cerebral edema and neurological dysfuncction. These lesions were significantly

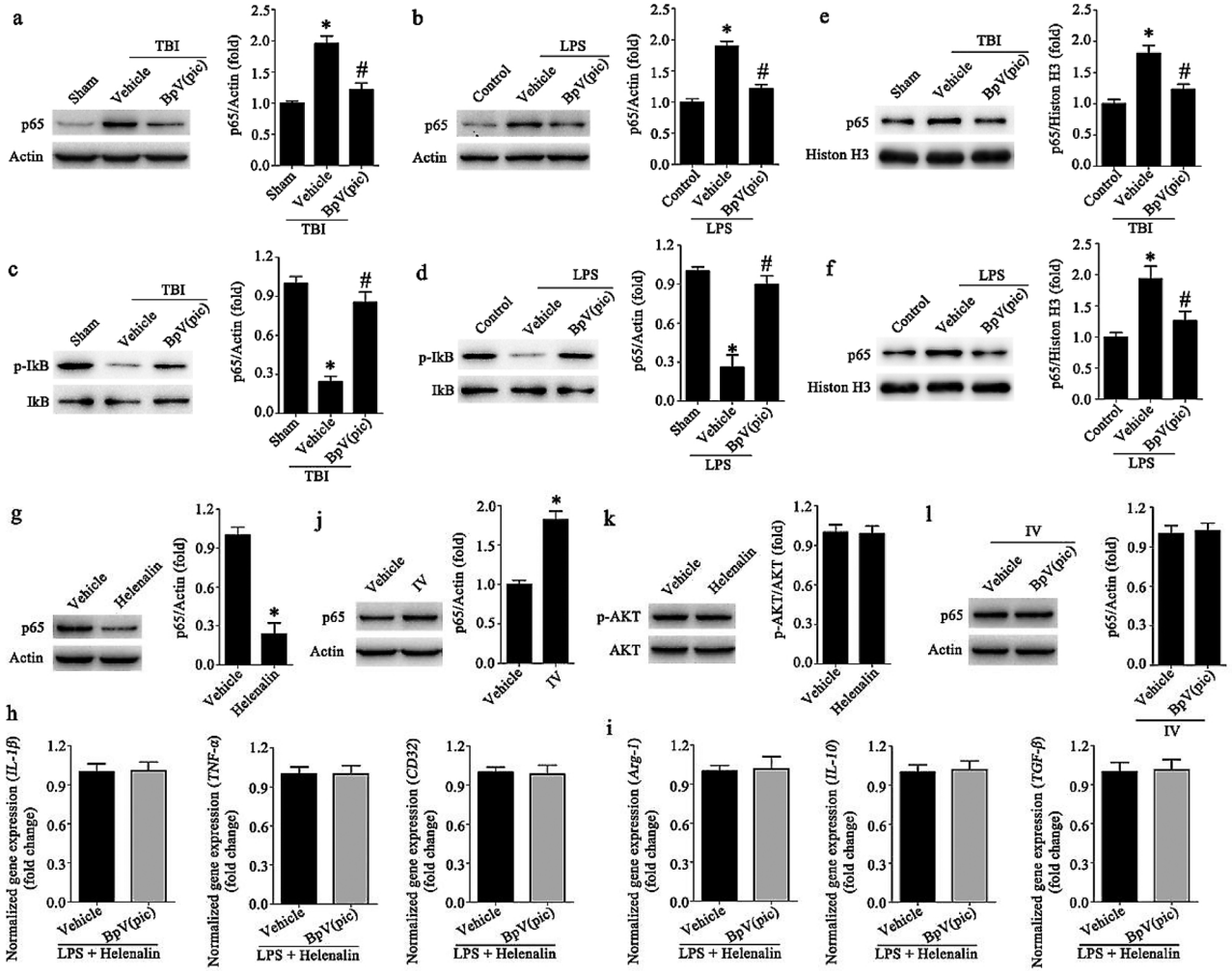

Fig. 5. NF-κB p65 mediates bpV(pic)-regulated neuroinflammation.
(a) Western blotting analysis of p65 showed that the level of p65 increased after TBI and inhibited by bpV(pic) treatment (n = 6 at each time point, $^{*}P < 0.05$ versus Sham, $^{\#}P < 0.05$ versus TBI + Vehicle). (b) Western blotting analysis of p65 in cultured cortical microglia (n = 6 at each time point, $^{*}P < 0.05$ versus Control, $^{\#}P < 0.05$ versus LPS + Vehicle). (c and d) Western blotting analysis of p-IkB in rats or cultured cortical microglia (n = 6 at each time point, $^{*}P < 0.05$ versus Control, $^{\#}P < 0.05$ versus LPS + Vehicle). (e and f) Western blotting analysis of the nucleus p65 in rats or cultured cortical microglia after nuclear plasma separation (n = 6 at each time point, $^{*}P < 0.05$ versus Control, $^{\#}P < 0.05$ versus LPS + Vehicle). (g) Western blotting analysis of p65 in cultured cortical microglia after Helenalin treatment (n = 6 at each time point, $^{*}P < 0.05$ versus Vehicle). (h and i) qRT-PCR analysis of M1 and M2 microglial markers in cultured cortical microglia after treatment of Helenalin ± BpV(pic) (n = 6 at each time point). (j) Western blotting analysis of p65 in cultured cortical microglia after IV treatment (n = 6 at each time point, $^{*}P < 0.05$ versus Vehicle). (k) Western blotting analysis of p-AKT in cultured cortical microglia after Helenalin treatment (n = 6 at each time point). (l) Western blotting analysis of p65 in cultured cortical microglia after treatment of IV ± BpV(pic) (n = 6 at each time point). Datas are expressed as mean ± SE. Statistical analysis was implemented by student's *t*-test and variance analysis.

observed in rats after TBI (Narayan et al., 2002). After treatment of bpV (pic), we found that TBI-induced increases in brain water content and neurological severity were significantly improved and bpV(pic) therefore exhibits a neuroprotective effect in TBI rats. Although the study design was that of a pre-treatment strategy and thus does not recapitulate human TBI scenarios, previously studies have shown that BpV(pic) is also neuroprotective when administered postoperatively in the ischemic stroke model (Liu et al., 2018; Zhang et al., 2017). The function of bpV(pic) is to inhibit the lipid phoaphatase activity of PTEN (Chen et al., 2015). PTEN lipid phosphatase activity negatively regulates AKT activation via the PI3K signaling pathway. The level of S473 phospharylation of AKT decreases after TBI in rats and BpV(pic) treatment up-regulates p-AKT levels. Meanwhile, in the case of pre-treatment inhibition of AKT, we found that the observed beneficial effects of bpV(pic) in edema and functional revovery are no longer observed. These results indicated that bpV(pic)-induced neuroprotection is mediated by AKT activation.

The inflammatory response is thought to be a key factor in the cascade of secondary injury after TBI. Microglia is the innate immune cell of the central nervous system and are the major mediators of neuroinflammation (Skaper et al., 2014). Microglia can be activated in the case of injury stimuli (Tsuda, 2016). Activated microglia have two phenotypes: classically activated (M1) and alternatively activeted (M2) (Szulzewsky et al., 2015). M1 and M2 microglia represent pro-inflammatory and anti-inflammatory, respectively (Pan et al., 2015). 24 h after TBI, microglia significantly polarizes to the M1 phenotype and expresses a large number of pro-inflammatory related factors. BpV(pic) treatment suppresses TBI-induced M1 microglia polarization and promotes anti-inflammatory. Previous studies have shown that AKT is a major regulator of neuroinflammation (Li et al., 2015). We confirm that bpV(pic)-mediated microglia polarization is depedent on AKT activation *in vivo* and *in vitro*. Meanwhile, NF-κB p65 have been reported to be a potential downstream of AKT-mediated inflammation. Our results show that the level of NF-κB p65 can be negatively regulated by bpV (pic), which mediates bpV(pic)-regulated neuroinflammation. BpV(pic) down-regulates NF-κB p65 by activating AKT, which in turn inhibits M1

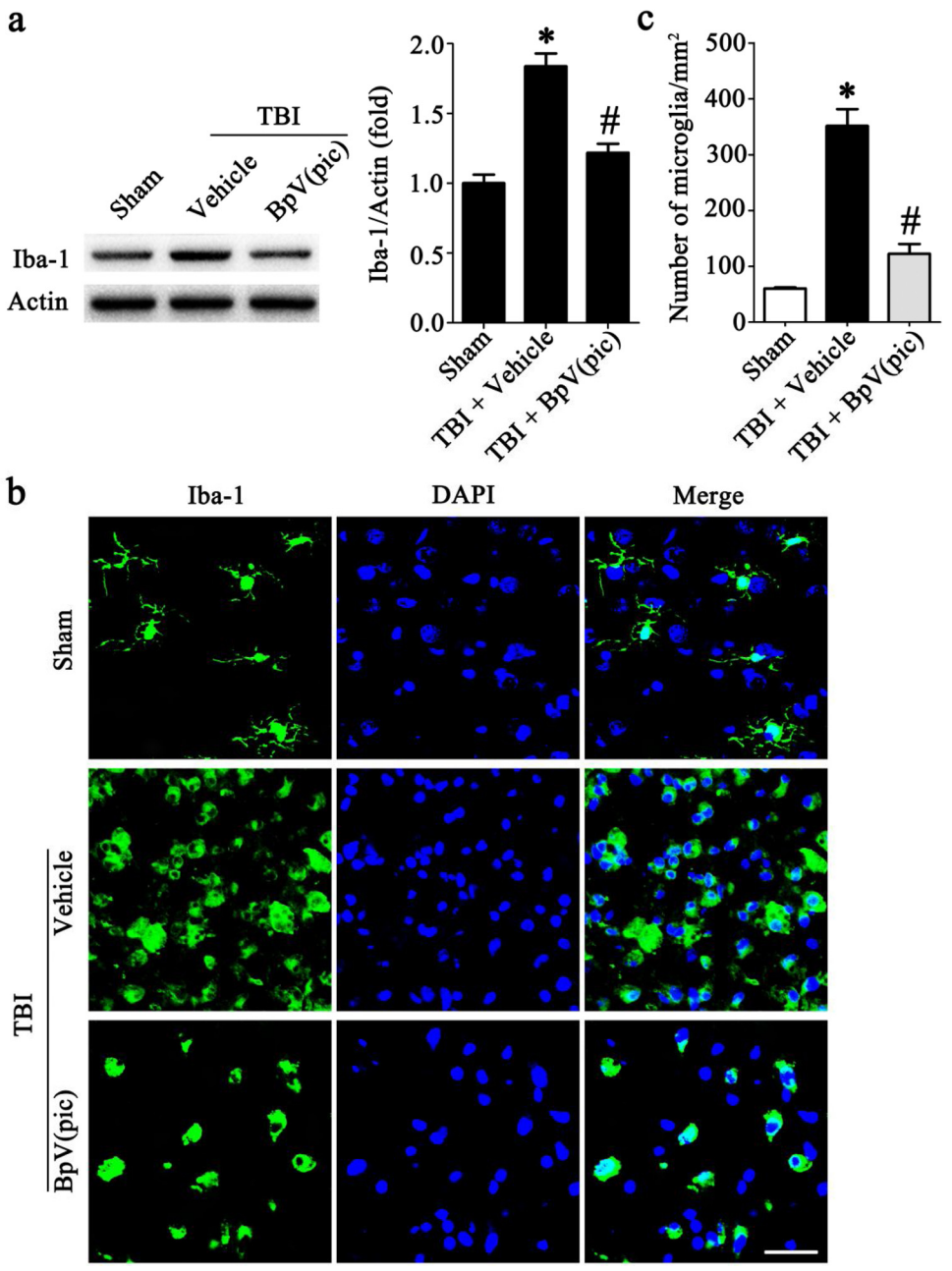

Fig. 6. BpV(pic) alleviates the increase of microglia in TBI lesion region.
(a) Western blotting analysis of Iba-1 showed that the level of Iba-1 increased after TBI and inhibited by bpV(pic) treatment (n = 6 at each time point, $^{*}P < 0.05$ versus Sham, $^{\#}P < 0.05$ versus TBI + Vehicle). (b and c) Immunofluorescence staining of Iba-1 (b) and quantitative analysis (c) showed that the number of microglia increased in peri-TBI region after TBI and bpV(pic) treatment inhibited this process (n = 6 at each time point, $^{*}P < 0.05$ versus Sham, $^{\#}P < 0.05$ versus TBI + Vehicle). Datas are expressed as mean ± SE. Statistical analysis was implemented by student's *t*-test and variance analysis.

microglial polarization after TBI.

Following TBI, there is an increase in inflammatory cells such as microglia in the injured area (Karve et al., 2016; Loane and Kumar, 2016). We found that bpV(pic) alleviates the increase of microglia seen in TBI lesions, and thereby indirectly reduces the inflammatory response. MCP-1, also called CCL2, a member of the CC family of chemokines, is known to recruit monocytes and macrophages to promote inflammation (Schneider et al., 2013). When MCP-1 is secreted, it causes a cascade reaction by acting with the receptor CCR2 on the cell membrane, causing inflammation or inflammatory cell migration (Guo et al., 2014). We show that MCP-1 is up-regulated after TBI and is reduced following bpV(pic) treatment. We also demonstrate that bpV (pic)-regulated MCP-1 expression is mediated by AKT/NF-κB p65 signaling pathway.

In conclusion, the present study demonstrates that bpV(pic) exhibits neuroprotection in TBI lesions and this process is mediated by AKT activation. BpV(pic) inhibits NF-κB p65 by activating AKT and subsequently suppresses a TBI-induced pro-inflammatory state, which in turn confers neuroprotective effects. Furthermore, the increase of microglia in the peri-TBI region can also be alleviated by bpV(pic) treatment, which may be achieved by bpV(pic)-mediated MCP-1 expression. Taken together, we identify a molecular mechanism by which the bpV(pic) negatively regulates neuroinflammation in conferring neuroprotection after rat TBI.

Author disclosure

We confirm that there are no conflicts of interest associated with this publication.

Acknowledgements

This work was supported by China Key Project of Basic Research ("973" Project; 2014CB541606), Natural Science Foundation of China (NSFC; 81470599) and The Fund of Collaborative Innovation Center for Brain Science to Q.W.

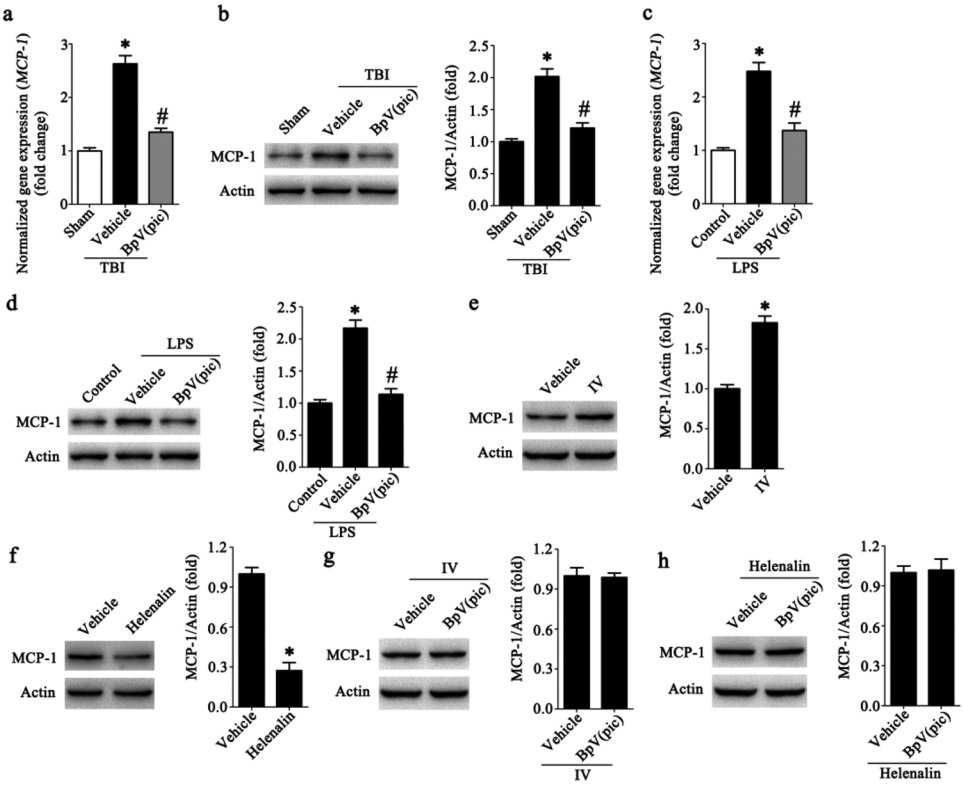

Fig. 7. BpV(pic) inhibits TBI-induced MCP-1 expression by regulation of AKT/NF-κB p65 signaling pathway.
(a) qRT-PCR analysis of *MCP-1* mRNA levels in rats after TBI (n = 6 at each time point, $^{*}P < 0.05$ versus Sham, $^{\#}P < 0.05$ versus TBI + Vehicle). (b) Western blotting analysis of MCP-1 showed that the level of MCP-1 increased after TBI and inhibited by bpV(pic) treatment (n = 6 at each time point, $^{*}P < 0.05$ versus Sham, $^{\#}P < 0.05$ versus TBI + Vehicle). (c) qRT-PCR analysis of *MCP-1* mRNA levels in cultured cortical microglia after LPS treatment (n = 6 at each time point, $^{*}P < 0.05$ versus Control, $^{\#}P < 0.05$ versus LPS + Vehicle). (d) Western blotting analysis of MCP-1 showed that the level of MCP-1 increased after LPS treatment and inhibited by bpV(pic) (n = 6 at each time point, $^{*}P < 0.05$ versus Control, $^{\#}P < 0.05$ versus LPS + Vehicle).(e) Western blotting analysis of MCP-1 in cultured cortical microglia after IV treatment (n = 6 at each time point, $^{*}P < 0.05$ versus Vehicle). (f) Western blotting analysis of MCP-1 in cultured cortical microglia after Helenalin treatment (n = 6 at each time point, $^{*}P < 0.05$ versus Vehicle). (g) Western blotting analysis of MCP-1 in cultured cortical microglia after treatment of IV ± BpV(pic) (n = 6 at each time point). (h) Western blotting analysis of MCP-1 in cultured cortical microglia after treatment of Helenalin ± BpV(pic) (n = 6 at each time point). Datas are expressed as mean ± SE. Statistical analysis was implemented by student's *t*-test and variance analysis.

Appendix A. Supplementary data

Supplementary material related to this article can be found, in the online version, at doi:https://doi.org/10.1016/j.molimm.2019.04.010.

References

Benson, M.J., Manzanero, S., Borges, K., 2015. Complex alterations in microglial M1/M2 markers during the development of epilepsy in two mouse models. Epilepsia 56 (6), 895–905.

Bromley-Brits, K., Deng, Y., Song, W., 2011. Morris water maze test for learning and memory deficits in Alzheimer's disease model mice. J. Vis. Exp. 53.

Chen, J., et al., 2001. Intravenous administration of human umbilical cord blood reduces behavioral deficits after stroke in rats. Stroke 32 (11), 2682–2688.

Chen, Y., et al., 2015. Administration of a PTEN inhibitor BPV(pic) attenuates early brain injury via modulating AMPA receptor subunits after subarachnoid hemorrhage in rats. Neurosci. Lett. 588, 131–136.

Chen, J., et al., 2016. Glycine confers neuroprotection through microRNA-301a/PTEN signaling. Mol. Brain 9 (1), 59.

Chen, J., et al., 2017a. A non-ionotropic activity of NMDA receptors contributes to glycine-induced neuroprotection in cerebral ischemia-reperfusion injury. Sci. Rep. 7 (1), 3575.

Chen, X., et al., 2017b. Omega-3 polyunsaturated fatty acid supplementation attenuates microglial-induced inflammation by inhibiting the HMGB1/TLR4/NF-kappaB pathway following experimental traumatic brain injury. J. Neuroinflammation 14 (1), 143.

Corrigan, F., Mander, K.A., Leonard, A.V., Vink, R., 2016. Neurogenic inflammation after traumatic brain injury and its potentiation of classical inflammation. J. Neuroinflammation 13 (1), 264.

Czeh, M., Gressens, P., Kaindl, A.M., 2011. The yin and yang of microglia. Dev. Neurosci. 33 (3–4), 199–209.

Feeney, D.M., Boyeson, M.G., Linn, R.T., Murray, H.M., Dail, W.G., 1981. Responses to cortical injury: I. Methodology and local effects of contusions in the rat. Brain Res. 211 (1), 67–77.

Guadagno, J., Swan, P., Shaikh, R., Cregan, S.P., 2015. Microglia-derived IL-1beta triggers p53-mediated cell cycle arrest and apoptosis in neural precursor cells. Cell Death Dis. 6, e1779.

Guo, Y.Q., et al., 2014. Expression of CCL2 and CCR2 in the hippocampus and the interventional roles of propofol in rat cerebral ischemia/reperfusion. Exp. Ther. Med. 8 (2), 657–661.

Karve, I.P., Taylor, J.M., Crack, P.J., 2016. The contribution of astrocytes and microglia to traumatic brain injury. Br. J. Pharmacol. 173 (4), 692–702.

Kumar, A., Loane, D.J., 2012. Neuroinflammation after traumatic brain injury: opportunities for therapeutic intervention. Brain Behav. Immun. 26 (8), 1191–1201.

Li, L., et al., 2015. G-CSF attenuates neuroinflammation and stabilizes the blood-brain barrier via the PI3K/Akt/GSK-3beta signaling pathway following neonatal hypoxia-ischemia in rats. Exp. Neurol. 272, 135–144.

Liu, B., et al., 2010. Preservation of GABAA receptor function by PTEN inhibition protects against neuronal death in ischemic stroke. Stroke 41 (5), 1018–1026.

Liu, X.Y., Zhang, L.J., Chen, Z., Liu, L.B., 2017. The PTEN inhibitor bpV(pic) promotes neuroprotection against amyloid beta-peptide (25-35)-induced oxidative stress and neurotoxicity. Neurol. Res. 39 (8), 758–765.

Liu, R., et al., 2018. ERK 1/2 activation mediates the neuroprotective effect of BpV(pic) in focal cerebral ischemia-reperfusion injury. Neurochem. Res.

Loane, D.J., Kumar, A., 2016. Microglia in the TBI brain: the good, the bad, and the dysregulated. Exp. Neurol. 275 (Pt 3), 316–327.

Majkutewicz, I., et al., 2016. Dimethyl fumarate attenuates intracerebroventricular streptozotocin-induced spatial memory impairment and hippocampal neurodegeneration in rats. Behav. Brain Res. 308, 24–37.

Makker, A., Goel, M.M., Mahdi, A.A., 2014. PI3K/PTEN/Akt and TSC/mTOR signaling pathways, ovarian dysfunction, and infertility: an update. J. Mol. Endocrinol. 53 (3), R103–R118.

Mason, D.Y., Micklem, K., Jones, M., 2000. Double immunofluorescence labelling of routinely processed paraffin sections. J. Pathol. 191 (4), 452–461.

Milella, M., et al., 2015. PTEN: multiple functions in human malignant tumors. Front. Oncol. 5, 24.

Muniyan, S., Ingersoll, M.A., Batra, S.K., Lin, M.F., 2014. Cellular prostatic acid phosphatase, a PTEN-functional homologue in prostate epithelia, functions as a prostate-specific tumor suppressor. Biochim. Biophys. Acta 1846 (1), 88–98.

Narayan, R.K., et al., 2002. Clinical trials in head injury. J. Neurotrauma 19 (5), 503–557.

Pan, J., et al., 2015. Malibatol a regulates microglia M1/M2 polarization in experimental stroke in a PPARgamma-dependent manner. J. Neuroinflammation 12, 51.

Poon, J.S., Eves, R., Mak, A.S., 2010. Both lipid- and protein-phosphatase activities of PTEN contribute to the p53-PTEN anti-invasion pathway. Cell Cycle 9 (22), 4450–4454.

Rhodes, J., 2011. Peripheral immune cells in the pathology of traumatic brain injury? Curr. Opin. Crit. Care 17 (2), 122–130.

Sawyer, A.J., et al., 2014. The effect of inflammatory cell-derived MCP-1 loss on neuronal survival during chronic neuroinflammation. Biomaterials 35 (25), 6698–6706.

Schneider, D., et al., 2013. Macrophage/epithelial cell CCL2 contributes to rhinovirus-

induced hyperresponsiveness and inflammation in a mouse model of allergic airways disease. Am. J. Physiol. Lung Cell Mol. Physiol. 304 (3), L162–L169.
Shi, G.D., et al., 2011. PTEN deletion prevents ischemic brain injury by activating the mTOR signaling pathway. Biochem. Biophys. Res. Commun. 404 (4), 941–945.
Skaper, S.D., Facci, L., Giusti, P., 2014. Neuroinflammation, microglia and mast cells in the pathophysiology of neurocognitive disorders: a review. CNS Neurol. Disord. Drug Targets 13 (10), 1654–1666.
Szulzewsky, F., et al., 2015. Glioma-associated microglia/macrophages display an expression profile different from M1 and M2 polarization and highly express Gpnmb and Spp1. PLoS One 10 (2), e0116644.
Tam, W.Y., Ma, C.H., 2014. Bipolar/rod-shaped microglia are proliferating microglia with distinct M1/M2 phenotypes. Sci. Rep. 4, 7279.
Tian, Y., Daoud, A., Shang, J., 2012. Effects of bpV(pic) and bpV(phen) on H9c2 cardiomyoblasts during both hypoxia/reoxygenation and H2O2-induced injuries. Mol. Med. Rep. 5 (3), 852–858.
Tsuda, M., 2016. Microglia in the spinal cord and neuropathic pain. J. Diabetes Investig. 7 (1), 17–26.
Wang, G.H., et al., 2011. Free-radical scavenger edaravone treatment confers neuroprotection against traumatic brain injury in rats. J. Neurotrauma 28 (10), 2123–2134.
Wang, X., Huang, H., Young, K.H., 2015. The PTEN tumor suppressor gene and its role in lymphoma pathogenesis. Aging (Albany NY) 7 (12), 1032–10349.
Xiong, Y., Mahmood, A., Chopp, M., 2010. Neurorestorative treatments for traumatic brain injury. Discov. Med. 10 (54), 434–442.
Xu, Y., et al., 2015. Telmisartan prevention of LPS-induced microglia activation involves M2 microglia polarization via CaMKKbeta-dependent AMPK activation. Brain Behav. Immun. 50, 298–313.
Yuan, F., et al., 2016. SIRT2 inhibition exacerbates neuroinflammation and blood-brain barrier disruption in experimental traumatic brain injury by enhancing NF-kappaB p65 acetylation and activation. J. Neurochem. 136 (3), 581–593.
Zhang, R., et al., 2012. An antitumor peptide from Musca domestica pupae (MATP) induces apoptosis in HepG2 cells through a JNK-mediated and Akt-mediated NF-kappaB pathway. Anticancer Drugs 23 (8), 827–835.
Zhang, C., et al., 2016. Corrigendum to "Neuroprotective and anti-apoptotic effects of valproic acid on adult rat cerebral cortex through ERK and Akt signaling pathway at acute phase of traumatic brain injury" [Brain Res.1555 (2014, Mar. 25) 1-9]. Brain Res. 1650, 283.
Zhang, Z.-F., et al., 2017. Bisperoxovandium (pyridin-2-squaramide) targets both PTEN and ERK1/2 to confer neuroprotection. Br. J. Pharmacol. 174 (8), 641–656.